

We are IntechOpen, the world's leading publisher of Open Access books Built by scientists, for scientists

6,900

Open access books available

186,000

International authors and editors

200M

Downloads

Our authors are among the

154

Countries delivered to

TOP 1%

most cited scientists

12.2%

Contributors from top 500 universities



WEB OF SCIENCE™

Selection of our books indexed in the Book Citation Index
in Web of Science™ Core Collection (BKCI)

Interested in publishing with us?
Contact book.department@intechopen.com

Numbers displayed above are based on latest data collected.
For more information visit www.intechopen.com



The Analysis and Optimization in Virtual Environment of the Mechatronic Tracking Systems used for Improving the Photovoltaic Conversion

Cătălin Alexandru and Claudiu Pozna
*University Transilvania of Braşov
Romania*

1. Introduction

The chapter presents researches in the field of increasing the efficiency of the solar energy conversion in electric energy, using tracking systems that change the position of the photovoltaic (PV) panel in order to maximize the solar radiation degree of use. From efficiency and safety point of view, we have selected a dual-axis equatorial tracking system, with two degrees of freedom. The both motions (daily and seasonal) are driven by rotary actuators, which integrate irreversible transmission for blocking the system in the intermediary positions, between actuatings.

The tracking system is approached in mechatronic concept, by integrating the electronic control system in the mechanical structure of the solar tracker. In this way, two main aspects are taken into consideration: optimizing the interaction between the mechatronic system components (the mechanic structure, and the control system); reducing the cost and time for the design process by replacing the traditional tests on hardware models, which are very expensive, with the testing in virtual environment. The study is performed by developing the virtual prototype of the mechatronic tracking system, which is a complex dynamical model. In fact, the virtual prototype is a control loop composed by the multi-body mechanical model connected with the dynamic model of the actuators and with the controller dynamical model. Using the virtual prototype, we are able to optimize the tracking mechanism, choose the appropriate actuators, and design the optimal controller.

The functionality of the tracking systems is evaluated from kinematic and dynamic point of view (i.e. motions, forces), as well as from energetic balance point of view. The key word of the design is the energetically efficiency. Using the tracking system, the PV panel follows the Sun and increase the collected energy, but the driving actuators consume a part of this energy. In order to analyze our solution, we will compare the PV system with tracking with a fixed panel, in standard testing conditions. One of the most important advantages of this kind of simulation is the possibility to perform measurements in any point and/or area of the system and for any parameter. This helps us to make quick decisions on any design changes without going through expensive prototype building and testing.

Source: Motion Control, Book edited by: Federico Casolo,
ISBN 978-953-7619-55-8, pp. 580, January 2010, INTECH, Croatia, downloaded from SCIYO.COM

2. Actual knowledge stage & original contributions

The theme of the chapter belongs to a very important field: renewable sources for energy production - increasing the efficiency of the photovoltaic conversion. The researches in this field represent a priority at international level because provides viable alternatives to a series of major problems that humanity is facing: the limited and pollutant character of the fossil fuels, global warming or the greenhouse effect. The solution to these problems is the renewable energy, including the energy efficiency, the energy saving, and systems based on clean renewable energy sources, like sun, wind and water. The concept of sustainable development have been enounced for the first time in 1987, in the Brundland Commission Report, and subsequent adopted at the political level, so in the Conference for Development and Environment from Rio de Janeiro (1992) the participant countries have undertaken to develop national strategies for sustainable development - The Program Agenda 21.

The solar energy conversion is one of the most addressed topics in the fields of renewable energy systems. The present-day techniques allow converting the solar radiation in two basic forms of energy: thermal and electric energy. Likewise, there are additional fields that use the solar energy, for example the hydrogen technology. The technical solution for converting the solar energy in electricity is well-known: the photovoltaic (PV) conversion. The PV systems can deliver energy on large-scale to a competitive price is the conclusion of the European Commission for Energy, in the report "A Vision for Photovoltaic Technology for 2030 and Beyond" (2004). The report emphasizes as the development of advanced technologies in the photovoltaic area, and a European strong and competitive industry will support the strategic initiatives concerning to the security and the diversity of the electric energy sources.

The efficiency of the PV systems depends on the degree of use and conversion of the solar radiation. The energy balance refers to the surface that absorbs the incoming radiation and to the balance between energy inflow and energy outflow. The rate of useful energy leaving the absorber is given by the difference between the rate of incident radiation on absorber and the rate of energy loss from the absorber (Goswami et al., 2000; Tiwari, 2002). The degree of use of the solar radiation can be maximized by use of mechanical systems for the orientation of the PV panels in accordance with the paths of the Sun. Basically the tracking systems are mechanical systems that integrate mechanics, electronics, and information technology. These mechanisms are driven by rotary motors or linear actuators, which are controlled in order to ensure the optimal positioning of the panel relatively to the Sun position on the sky dome, on the entire period of the day (the daily motion, from East to West), and also depending on the season (the seasonal/elevation motion). The orientation of the photovoltaic panels may increase the efficiency of the conversion system from 20% up to 50% (Abdallah & Nijmeh, 2004; Canova et al., 2007; Hoffmann et al., 2008).

In literature, the increasing of the photovoltaic efficiency is approached mainly through the optimization of the conversion to the absorber level, and this because the subject is mainly specific for the chemical and electrical engineering. In our vision, this is an interdisciplinary field that concentrates the competences of three fundamental domains: chemical, electrical, and mechanical. The solar energy conversion field interferes with the mechanical engineering there where the optimization process of the conversion uses tracking systems based on mechatronic devices (the maximum degree of collecting is obtained when the solar radiation is normal on the active surface).

Having in view the operating principle, there are two fundamentals types of tracking systems: passive and active trackers. The passive trackers are based on thermal expansion of

a Freon-based liquid from one edge of the tracker to another because of the heat sensitive working fluid (Clifford & Eastwood, 2004). The active trackers are based on electrically operated positioning drives, which need motors, gearboxes, mechanisms, couplings etc. Usually, the nowadays active tracking systems are based on planar or spatial linkages, gears, chain and belt transmissions.

The photovoltaic system with tracking is efficient if the following condition is achieved:

$$\varepsilon = (E_T - E_F) - E_C \gg 0 \quad (1)$$

in which E_T is the electric energy produced by the photovoltaic panel with tracking, E_F - the energy produced by the same panel without tracking (fixed), and E_C - the energy consumption for orienting the PV panel. In the current conditions, the maximization of the efficiency parameter ε , by the optimization of the tracking system, became an important challenge in the modern research and technology.

In the design process of the tracking systems, the solar radiation represents the main input data. Interacting with atmospheric phenomena involving reflection, scattering, and absorption of radiation, the quantity of solar energy that reaches the earth's surface is reduced in intensity. The total solar radiation received at ground level includes two main components: direct solar radiation and diffuse radiation (Meliß, 1997). The solar radiation can be measured using traditional instruments, or can be digitally recorded with a data acquisition system. Within an EU funded project, a solar radiation atlas was realized for Europe (Scharmer & Greif, 2000). At the same time, there were developed large meteorological databases, such as Meteonorm - Global Meteorological Database for Engineers, Planners and Education. In addition, different models were developed for estimating the solar radiation. The traditional Angstrom's linear approach is based on measurements of sunshine duration, while relatively new methods are based on artificial neural networks - ANN (Tymvios et al., 2005). Different models for estimating the monthly mean solar radiation, including linear Angstrom-Prescot variation, quadratic equation, logarithmic variation, and exponential function, are comparatively analyzed by using as principal element the root mean square error (Salmi et al., 2007). A step by step procedure was developed for implementing an algorithm to calculate the solar irradiation, using both zenith and azimuth angles to describe sky element's position, for a surface that is tilted to any horizontal and vertical angle (Reda & Andreas, 2004).

Other papers refer to the computation of the yearly energy collection allowed by different tracking strategies. A theoretical analysis of different intervals of intermittent two-axis tracking of the Sun on the amount of annual energy received by solar panels was performed for estimating the solar radiation in standard sky condition (Koay & Bari, 1999). Using as input data the location latitude and commonly available values of monthly irradiation, a relation between the latitude of the chosen location and the most suitable tracker was established (Sorichetti & Perpignan, 2007). For comparing the energy capture between fixed tilt angle and sun trackers, in clear sky and mean sky conditions, the Moon-Spencer and the Aste models are frequently used (Canova et al., 2007). Specific software tools were also developed to simulate the energy yield of PV systems as a function of the ground cover ratio, for different tracking strategies (Narvarte & Lorenzo, 2007).

The active tracking systems contain mechanisms, which are driven by controlled motors - actuators. Regarding the control process, in literature, closed loop systems with photo sensors are traditionally used. The photo sensors are responsible for discrimination of the

Sun position and for sending electrical signals, proportional with the error, to the controller, which actuates the motors to track the Sun. Many authors have adopted this method as a basis in construction and design of such systems (Baltas et al., 1986; Dobon et al., 2003; Karimov et al., 2005). Although, the orientation based on the Sun detecting sensors, may introduce errors in detection of real sun position for variable weather conditions.

The alternative consists in the opened loop systems (Abdallah & Nijmeh, 2004; Alexandru & Pozna, 2008; Roth et al., 2004), which are based on mathematic algorithms/programs that may provide predefined parameters for the motors, depending on the sun positions on the sky dome (i.e. the astronomic movements of the Sun - Earth system). These positions can be precisely determined because they are functions of the solar angles that can be calculated for any local area. By using this control technique, based on predefined parameters, the errors introduced by the use of the sensors may be avoided.

Other solution is to incorporate some kind of Sun position sensor to check and calibrate automatically the astronomical control system. In addition, the tracking system can also be adjusted to provide maximum output energy, to self-trim it initially or self correct itself throughout its life (Sala et al., 2002). Such hybrid control system consists of a combination of opened loop tracking strategies, based on solar movement models, and closed loop strategies, using dynamic feedback controller (Rubio et al., 2007).

From the controller point of view, different control strategies are used, such as classical techniques as PID algorithm or more advanced strategy such as fuzzy logic controller - FLC. The design of a low cost two-axis solar tracker for obtaining a high precision positioning of the PV panel is made considering a control-board that is able to support different PID and FLC control strategies (Yazidi et al., 2006). An evolution of the fuzzy control concept is the fuzzy logic neural controller (FNLC), which allows the PV system to learn control rules (Chojnacki, 2005). A more complex controller incorporates the advantages of two alternate design techniques, namely the deadbeat regulator - for quick, rough control, and the LOG/LTR regulator - for soft final tracking (Rubio & Aracil, 1997). The first order Sugeno fuzzy inference system is used for modelling and designing the controller of an azimuth & elevation solar tracker (Alata et al., 2005); the estimation of the insolation incident on the two axis sun tracking system is determined by fuzzy IF-THEN rules.

The orientation principle of the photovoltaic panels is based on the input data referring to the position of the Sun on the sky dome. For the highest conversion efficiency, the sunrays have to fall normal on the receiver surface so the system must periodically modify its position in order to maintain this relation between the sunrays and the PV panel. The positions of the Sun on its path along the year represent input data for the design process of the tracking systems. The Earth describes along the year a rotational motion following an elliptical path around the Sun. During one day, the Earth also spins around its own axis describing a complete rotation that generates the sunrises and the sunsets. The variation of the altitude of the Sun on the celestial sphere during one year is determined by the precession motion, responsible for a declination of the Earth axis in consideration with the plane of the elliptic yearly path. In these conditions, for the design process of the tracking systems there are considered two rotational motions: the daily motion, and the yearly precession motion.

Consequently, there are two basic types of tracking systems (fig. 1): single-axis tracking systems (a), and dual-axis tracking systems (b, c). The single-axis tracking systems spins on their axis to track the Sun, facing east in the morning and west in the afternoon. The tilt angle of this axis equals the latitude angle of the loco because this axis has to be always

parallel with the polar axis. In consequence for this type of tracking system is necessary a seasonal tilt angle adjustment. The two-axis tracking systems combine two motions, so that they are able to follow very precisely the Sun path along the period of one year.

Depending on the relative position of the revolute axes, there are two types of dual-axis systems: polar (b), and azimuthal (c). For the polar trackers, there are two independent motions, because the daily motion is made rotating the PV panel around the polar axis. For the azimuthal trackers, the main motion is made by rotating the PV panel around the vertical axis, so that it is necessary to continuously combine the vertical rotation with an elevation motion around the horizontal axis.

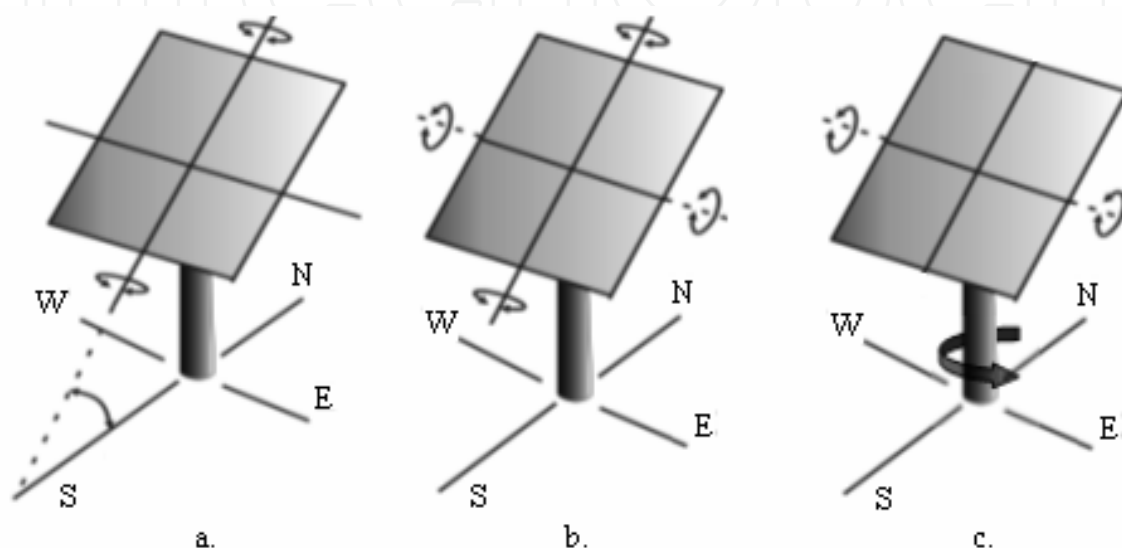


Fig. 1. Basic types of solar tracking systems

The research of the literature reveals the limits of the actual stage in the development of the mechanical device of the tracking systems. Since now there are no unitary modellings on structural, kinematical and dynamical aspects in designing the mechanical structure. At the same time, a general approaching for the conceptual design and the structural synthesis of these mechanisms is missing. Thus rises the necessity of a unitary modelling method of mechanisms, and in our opinion this method is the Multi Body Systems (MBS) method, which may facilitates the self-formulating algorithms (Garcia de Jalón & Bayo, 1994; Schiehlen, 1997). At the same time, in the reference literature, there were not identified compliant models of tracking systems that allow the precise simulation of the system behaviour with deformable components (bodies, joints); this is the reason for the missing of the studies concerning the vibratory and durability characteristics of the tracking systems.

On the other hand, the research is focused mostly on the quantity of the energy achieved by tracking and there is no evaluation on the energy consumption determined by the orientation (consumed energy by the motors/actuators). A possible cause of this case is due to the fact that the issue is not approached as an integrated assembly (mechanical device + actuating system and control). Thus, we propose the integration of the main components at the virtual prototype level, during the entire design process (i.e. the modelling in mechatronic concept), which allows at the same time the evaluation of the energy gain by orientation as well as the energetic consumption necessary for the motion.

In these terms, we can systematize the following scientific objectives of the paper: identifying & modelling the reference input data for the PV system design (i.e. the solar

radiation); conceptual design of the tracking mechanisms for identifying suitable solutions (from functional and constructive point of view); optimizing the tracking mechanisms from geometric point of view; in-detail modelling of the tracking mechanisms, including the friction and the deformability; developing the control strategies in order to obtain as much as possible incident radiation with minimum energy consumption; evaluating the vibratory characteristics; performing the energy balance (i.e. the energetic efficiency). In this way, the necessary conditions for approaching the functionality of the entire assembly (including the PV panel, the tracking mechanism, the motors, and the control system) are assured.

No less important there are the instruments (techniques) used for realizing the objectives, based on testing - simulation in the virtual environment (digital mock-up, virtual prototyping). This kind of approach is based on the design of the detailed digital models and the use of these in virtual experiments, by reproducing with the computer of the real phenomena. An important advantage of this process consists of the possibility to develop measurements in any point or zone and for any type of the parameter (motion, force, energy) that is not always possible to the experimental testing on the physical models (the missing of the adequate sensors or the misplace for these sensors, high temperatures etc.). The design process based on the virtual prototyping allows the fast evaluation of the shape, mounting and functions of the tracking systems, eliminating the large period amount necessary for physical prototyping, or very expensive design modifications.

3. Design tool - virtual prototyping platform

Traditional CAD/CAM/CAE practices used to evaluate the functional characteristics of the mechanical & mechatronic systems were focused on a concept referred to as art-to-part. Nearly all engineering software activity was oriented toward the design, development, and manufacturing of higher quality parts. Unfortunately, optimal part design rarely leads to optimal system design. The interaction of form, fit, function, and assembly of all parts in a product is a major contributor to overall product quality. The big opportunity to increase quality and reduce time and cost has now shifted to the system level (Ryan, 2001).

The system-focused approach involves the following software solutions: Digital Mock-Up (DMU) - to investigate product form and fit, Functional Virtual Prototyping (FVP) - to assess product function and operating performance, and Virtual Factory Simulation (VFS) - to assess assembly and manufacturability of the product. The integration of the system-focused tools provides a means for realizing the transition from physical to virtual prototyping, with all of the concomitant benefits.

The steps to create a virtual (software) prototype mirror the steps to build a physical (hardware) prototype (Haug et al., 1995). During the build phase, virtual prototypes are created of both the new product concept and any target products which may already exist in the market. The geometry and mass properties are obtained from component solid models. The structural, thermal and vibratory characteristics result from component finite element models or experimental tests.

One of the most important axioms for successful functional virtual prototyping is to simulate as test. Testing of hardware prototypes has traditionally involved both lab tests and field tests in various configurations, which are very expensive. With virtual prototyping, it is enough to create virtual equivalents of the lab and field tests.

To validate the virtual prototype, the physical and virtual models are tested identically, using the same testing and instrumentation procedures. The results are compared, and

design sensitivity analyses are performed to identify design parameters that have influence on the performance results that do not correspond. Afterwards, different changes on these parameters are realized in order to obtain an acceptable correlation.

Refining the virtual prototype involves the fidelity of the model. By replacing the rigid components with flexible counterparts, adding frictions, or representing the automatic systems that control the operating performance of the mechanical system can make the improvement of the virtual prototype.

The optimization of the virtual prototype is made with the following steps: parameterizing the model; defining the design variables; defining the objective functions for optimization and the design constraints; performing design studies and design of experiments; optimizing the model on the basis of the main design variables. Parameterizing the model simplifies changes to model because it helps to automatically size, relocate and orient bodies. Design variables allow creating independent parameters and tie modelling objects to them. Design study describes the ability to select a design variable, sweep that variable through a range of values and then simulate the motion behaviour of the various designs in order to understand the sensitivity of the overall system to these design variations.

The objective function of the optimization is a numerical quantification that distinguishes or rates candidate designs. The constraints are boundaries that directly or indirectly eliminate unacceptable designs; they often take the form of additional goals for the mechanism design. In general, the optimization problem is described as a problem to minimize or maximize the objective function over a selection of design variables, while satisfying various constraints on the design.

The analysis flow-chart of the tracking systems is shown in figure 2. The kinematic model of the tracking system contains the rigid parts, which are connected through geometric constraints (joints), and the specific geometric parameters; the input is made using kinematic restrictions (motion generators) that impose the motion of the driving elements (usually, the angular or linear positions). The aim of the kinematic analysis is to evaluate the relative motion between components, and to identify if the tracking system is able to generate the angular fields of the photovoltaic panel.

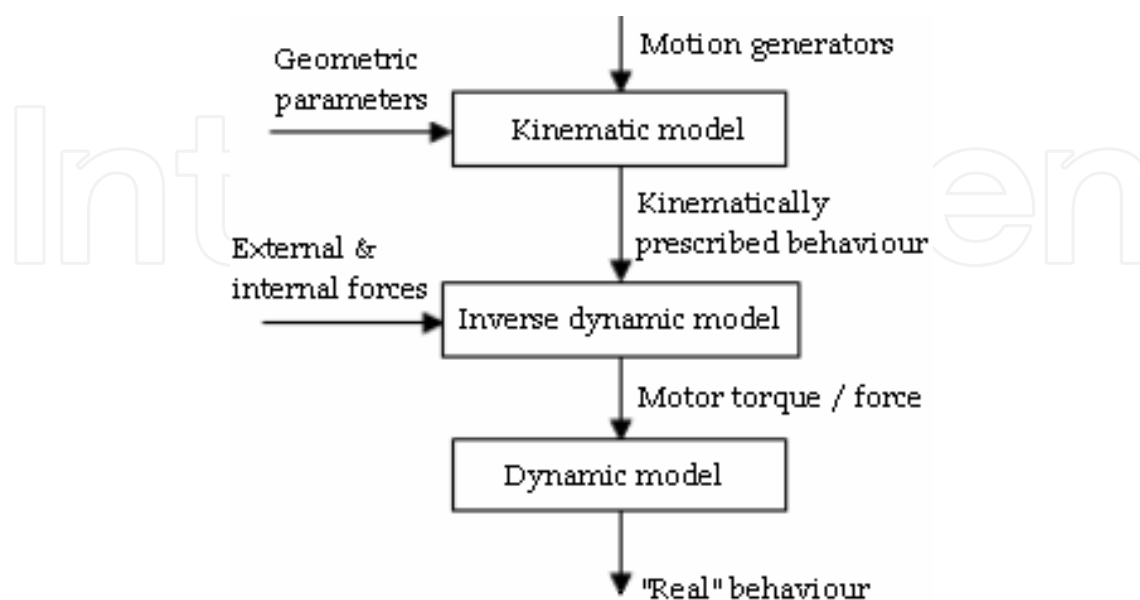


Fig. 2. The analysis flow-chart of the solar trackers

The inverse dynamic model includes the kinematic model and, in addition, the external and internal forces & torques. Basically, there are taken in consideration the mass forces, which depend on the geometric model and the material content for each mobile body, the friction forces, and the reactions in joints. In addition, the model can be completed with other external factors (perturbations), for example the wind or snow action. The aim of the inverse dynamic analysis is to determine the motor torque and/or the motor force applied by the driving element, in order to generate the cinematically-prescribed behaviour. The dynamic model of the tracking system (i.e. the virtual prototype) includes the components of the inverse dynamic model, but the input is made through the above-determined motor torques - forces; the goal is to evaluate the system's behaviour in real operating conditions.

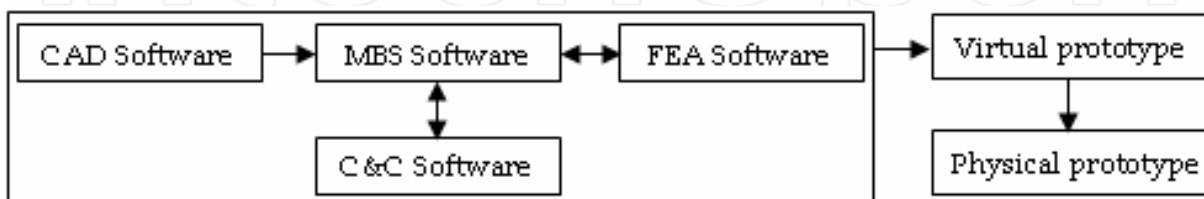


Fig. 3. Virtual (software) prototyping platform

Generally, the virtual prototyping platform, shown in figure 3, includes the following software products (Alexandru & Comsit, 2008): CAD - Computer Aided Design (ex. CATIA, PROENGINEER, SOLIDWORKS); MBS - MultiBody Systems (ex. ADAMS, SD-EXACT, DYMES); FEA - Finite Element Analysis (ex. NASTRAN, COSMOS, ANSYS); Command & Control (ex. MATLAB, EASY5). The MBS software, which is the main component of the platform, allows analyzing, optimizing, and simulating the system under real operating conditions. The CAD software is used for creating the geometric (solid) model of the mechanical system. This model contains data about the mass & inertia properties of the rigid parts. The part geometry can be exported from CAD to MBS using standard format files, such as IGS, DWG, DXF, STEP or PARASOLID. To import the geometry of the rigid parts, the MBS software reads the CAD file and converts the geometry into a set of MBS elements. The FEA software is used for modelling flexible bodies in mechanical systems. Integrating flexibilities into model allows to capture inertial and compliance effects during simulations, to study deformations of the flexible components, and to predict loads with greater accuracy, therefore achieving more realistic results. The flexible body characteristics are defined in a finite element modelling output file (MNF - Modal Neutral File). The information in a MNF includes location of nodes and node connectivity, nodal mass and inertia, mode shapes, generalized mass and stiffness for modal shapes. The MBS model transmits to FEA the motion & load states in the mechanical system, which can be defined using a FEA Loads format file.

In the modern concept, the mechanical systems are approached as mechatronic systems, which integrate mechanics, electronics, and information technology. The mechatronic systems are built-up with some units with basic functions, which are made to interact between them in order to form a complex system with a given functionality. Integrating the control system in the mechanical model at the virtual prototype level, the mechanical designer and the controls designer can share the same model; they can also verify from one database the combined effects of a control system on a nonlinear, non-rigid model. In this way, the physical testing process is greatly simplified, and the risk of the control law being poorly matched to the physical (hardware) prototype is eliminated. The C&C (Command &

Control) software directly exchanges information with the MBS software: the output from MBS is input for C&C and vice-versa. The mechanical model and the control system communicate by passing state variables back and forth. The analysis process creates a closed loop in which the control inputs from the control application affect the MBS simulation, and the MBS outputs affect the control input levels (Alexandru, 2008).

In this approach, complex virtual prototypes for different mechanical & mechatronic systems (including the renewable energy systems) can be developed, which exactly replicate the structure (components) and the operating conditions of the real physical products. For this paper, in order to develop the virtual prototype of the photovoltaic tracking system, we have used a digital prototyping platform that integrates the following software solutions: CAD - CATIA (to create the solid model, which contains information about the mass & inertia properties of the parts), MBS - ADAMS/View (to analyze, and optimize the mechanical device), C&C - ADAMS/Controls and MATLAB/Simulink (to create the control block diagram, and to simulate the mechatronic system), FEA - ADAMS/AutoFlex (for identifying the eigenshapes, eigenfrequencies and equivalent stresses of the system).

4. Developing the virtual prototype of the tracking system

For identifying accurate and efficient mechanical configurations suitable for tracking systems, a structural synthesis method based on the multi-body systems theory has been developed. The conceptual design can be performed in the following stages (Comsit & Visa, 2007): identifying all possible graphs, by considering the space motion of the system, the type of joints, the number of bodies, and the degree of mobility; selecting the graphs that are admitting supplementary conditions imposed by the specific utilization field; transforming the selected graphs into mechanisms by mentioning the fixed body and the function of the other bodies, identifying the distinct graphs versions based on the preceding particularizations, transforming these graphs versions into mechanisms by mentioning the types of geometric constraints (ex. revolute joint - R, or translational joint - T).

The graphs of the multibody system are defined as features based on the modules, considering the number of bodies and the relationships between them (e.g. R, T, R-R, R-T, RR-RR, RR-RT and so on. In this way, a collection of possible structural schemes have been obtained. In order to select the structural solution for study, we applied specific techniques for product design such as multi-criteria analysis and morphological analysis (Pahl & Beitz, 1996). The multi-criteria analysis was performed using the following steps: selecting the possible variants in accordance with the structural synthesis; establishing the evaluation criteria and the weight coefficient for each criterion (the FRISCO formula); granting the importance note to a criterion and computing the product between the importance note and the weight coefficient in the consequences matrix.

The evaluation criteria of the solutions were referring to the tracking precision, the amplitude of the motion, the complexity of the system, the possibility for manufacturing and implementation. The final solution has been established based on the morphological analysis, the description of possible solutions being conducted by combinatorial procedures that associates the requirements to be met (parameters, functions, attributes). In this way, there is described the morphological table, which eliminates the irrational constructive or incompatible solutions.

Using this conceptual design method, we established the solution for the tracking system in study, which is a polar dual-axis mechanism, the basic scheme being shown in Fig. 1,b. The

revolute axis of the daily motion is fixed and parallel with the polar axis. The both motions are directly driven by rotary motors, type MAXON ROBOTIS DX-117 (fig. 4). The motion is transmitted from the output shafts of the motors by using worm gears; these irreversible transmissions assure at the same time the blocking of the system in the stationary positions between actuations, when the motors are stopped (in this way, there is no energy consumption in the stationary positions).



Fig. 4. The rotary motor MAXON DX-117



Fig. 5. The MBS mechanical model of the dual-axis tracking mechanism

The “multibody system” model of the mechanism, developed by using the MBS environment ADAMS/View of MSC Software, it is designed so that it has three parts, as follows (fig. 5): base/sustaining frame (1), on which there is disposed the support of the motor and the fixed axle of the revolute joint for the daily motion - A; intermediary element (2), which includes the mobile parts of the joint A, and the fixed part of the joint for the seasonal motion - B; support part (3), which contains the axle of the seasonal motion, the panel frame, and the PV panel.

For developing the constructive solution of the tracking system, we used the CAD software CATIA of Dassault Systems. The geometry transfer from CATIA to ADAMS was made using the STEP (Standard for the Exchange of Product Model Data) file format, through the ADAMS/Exchange interface. The STEP format describes the level of product through a

specialized language (Express), which establishes the correspondence between the STEP file and the CAD model. The geometry of the PV panel corresponds to a VITOVOLT 200 panel, which has the following specifications: active surface - 1.26 m², weight - 15.5 Kg.

The virtual model takes into consideration the mass forces, the reaction in joints, and the joint frictions. The block diagram of the revolute joint is shown in figure 6, with the following notations: F_a , F_r - axial and radial joint reactions, T_r - bending moment, T_p - torque preload, T_f - frictional torque, R_n - friction arm, R_p - pin radius, R_b - bending reaction arm, μ - friction coefficient (static or dynamic), SW - switch block, MAG - magnitude block, ABS - absolute value block, FR - friction regime determination, \oplus - summing junction, \otimes - multiplication junction. Joint reactions, bending moment, and torque preload determine the frictional torque in a revolute joint. These force effects (one or more) can be turned-off by using switches. The joint reactions are converted into equivalent torques using the respective friction arm and pin radius. The joint bending moment is converted into an equivalent torque using pin radius divided by bending reaction arm. The joint bending moment is converted into an equivalent torque using pin radius divided by bending reaction arm.

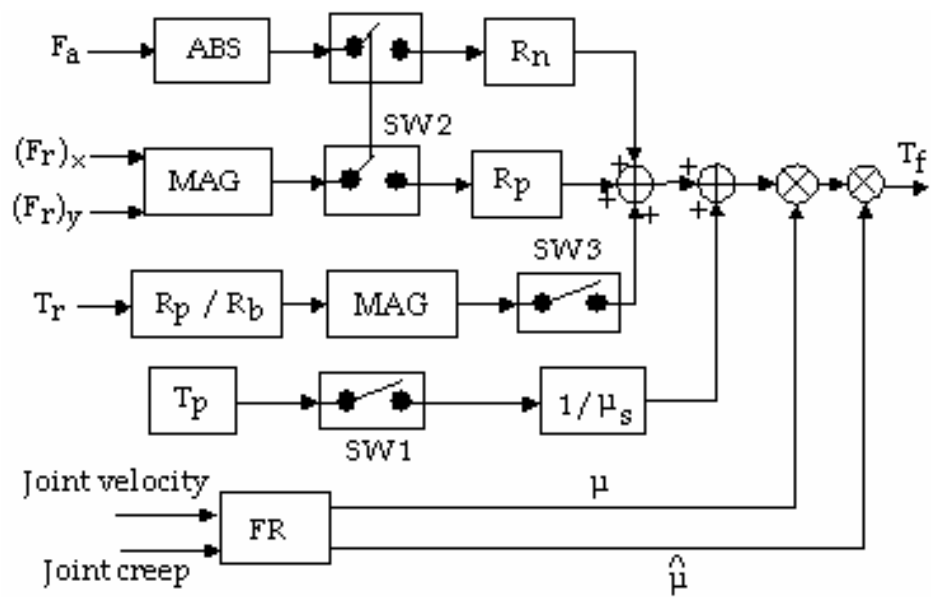


Fig. 6. The block diagram of the revolute joints

For simulating the real behaviour of the tracking system, in order to obtain more realistic results, we have developed the control system in the concurrent engineering concept, using ADAMS/Controls and MATLAB/Simulink. The solar tracker is an automated (controlled) system, which has as task the orientation of the PV panel (i.e. the effector) on the imposed trajectory. Generally, the solar tracking system is composed by different subsystems, whose structure is shown in figure 7. In these terms, for the polar solar tracker in study (see fig. 5), there are the following subsystems: the DC rotary actuators, the mechanical transmissions, and the mechanism's structure.

The connecting scheme of the subsystems emphasis the following: the mechanism is a coupled system (each element has influence on the others); the transmissions are connected between the joints and the DC motors; the transmissions and the DC motors are uncoupled subsystems. In figure 7,b there is shown a section through a certain joint "k" (in this case, $k=1, 2$). The design problem can be formulated in the following ways: designing a control system which allows the displacement of the effector on the imposed trajectory; because the imposed trajectory can be transformed, using the inverse kinematics, in $n=2$ imposed

trajectories for the motor axes, the objective is to design a control system which allows the rotation of the motor axes on the imposed trajectory.

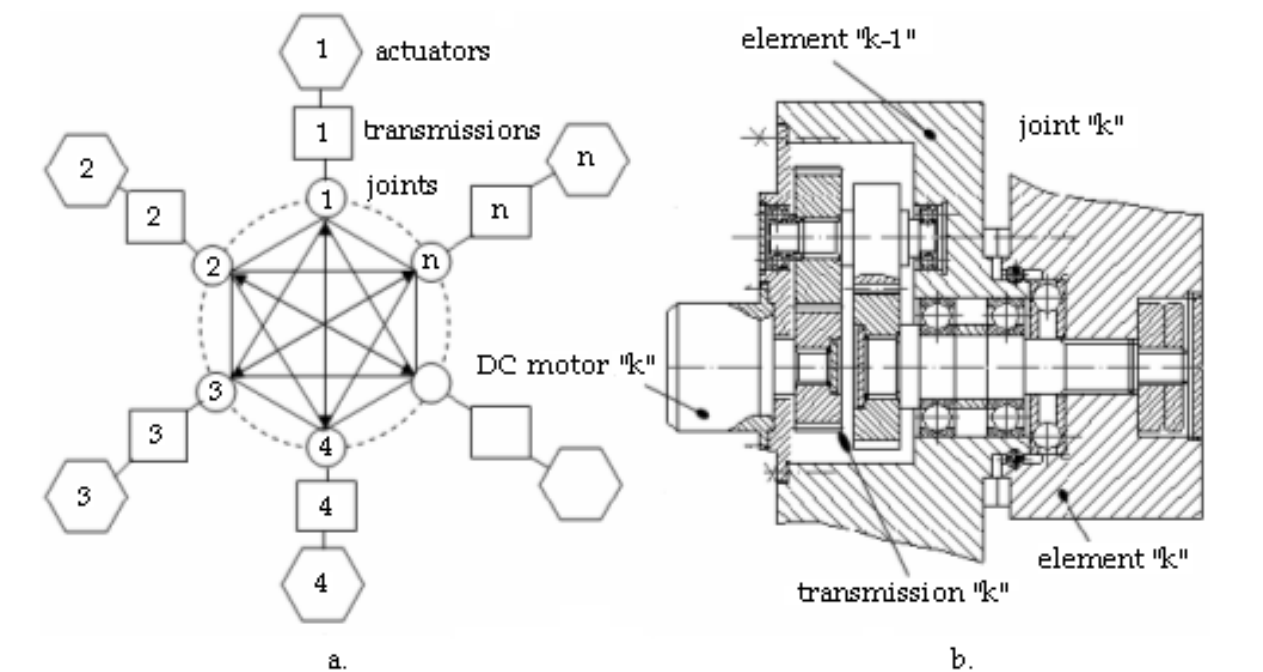


Fig. 7. The main subsystems of the solar tracker

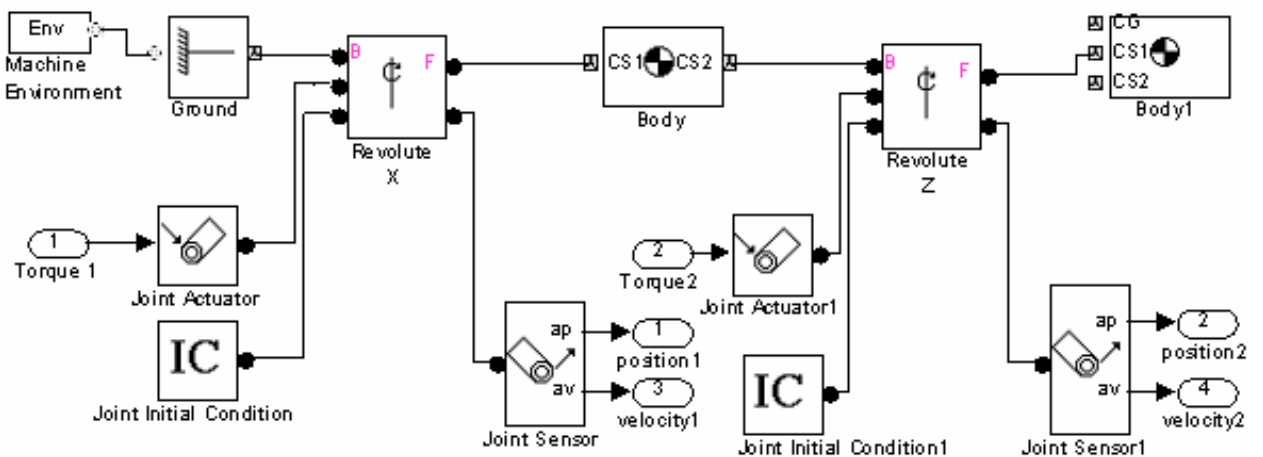


Fig. 8. The dynamic model of the solar tracker

The dynamic model of the polar tracking system is shown in figure 8, the MBS virtual prototype being the one in figure 5. The mechanical transmission is modeled with the following equations:

$$\begin{cases} q_{m1/2} = i_{1/2} \cdot q_{1/2} \\ T_{1/2} = \frac{1}{i_{1/2}} \cdot \tau_{1/2} \end{cases} \quad (2)$$

in which: $q_{1/2}$ is the angular position in the revolute joint; $q_{m1/2}$ - the angular position of the motor axis; $\tau_{1/2}$ - the torque in joint; $T_{1/2}$ - the motor torque; $i_{1/2}$ - the transmission ratio of the rotary motor.

The DC rotary motor, which is an electro-mechanical system, is modeled by the following relations (fig. 9):

$$V = R_a i + L \frac{di}{dt} + E, J \ddot{q}_m = K_M i - b \dot{q}_m - T, E = K_b \dot{q}_m$$

(3)

where V is the input voltage, T - the torque, R_a - the resistance, L - the inductance, i - the current, K_b - the contra-electromotor constant, q_m - the rotor position, \dot{q}_m - the angular velocity of the rotor (ω_m), J - the inertial moment, K_M - the motor torque coefficient, b - the viscous friction; the values of the specific parameters are presented in table 1.

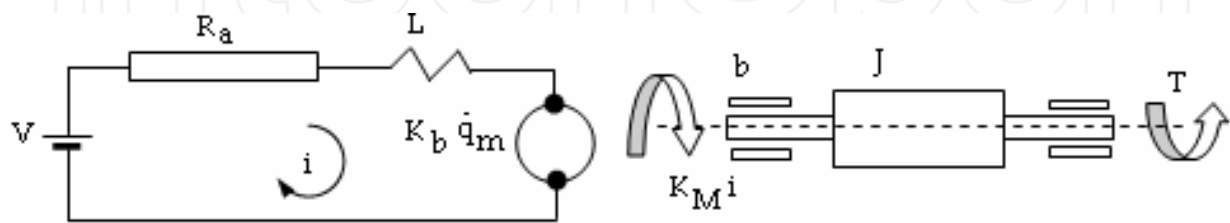


Fig. 9. The dynamic model of the DC motor

System	Parameter	1	2
Mechanical structure	m [kg]	0.7	0.5
	J [Nms ² /rad]	1.8e-3	0.78e-3
	l [m]	0.5	0.35
	c [m]	0.25	0.125
Transmission	i	150	150
DC motor	J [Nms ² /rad]	233e-6	
	L [H]	0.5	
	Ra [Ω]	0.8	
	b [Nms/rad]	0.1	
	K _M [Nm/amp]	176e-3	
	K _b [Vs/rad]	0.105	

Table 1. The numeric values of the motors’ parameters

The structural block scheme of the tracking system is shown in figure 10. There can be identified the connections between subsystems, and the measures which define the communications. According with this model, the goal is to control the DC motors (the reference measures of the control problem are the revolution angles of the motor axes $q_{1/2}$), which are perturbed with the torques $T_{1/2}$. The torques computation is based on the dynamic model of the mechanical structure on which acts outside forces.

For detailing the previous diagram, we will focus on the DC motors subsystems, and will transform the equations (3) with the Laplace operator:

$$Q_m(s) = G_V(s) \cdot V(s) + G_T(s) \cdot T(s)$$

(4)

in which $\Omega_m(s)$ is the Laplace transform of ω_m , $V(s)$ - the Laplace transform of V , $T(s)$ - the Laplace transform of T , $G_V(s)$ & $G_T(s)$ - the transfer functions:

$$G_V(s)=\frac{K_M}{LJs^3+(JRa+bL)s^2+(bRa+K_bK_M)s},\;G_T(s)=\frac{Ls+Ra}{LJs^3+(JRa+bL)s^2+(bRa+K_bK_M)s}\tag{5}$$

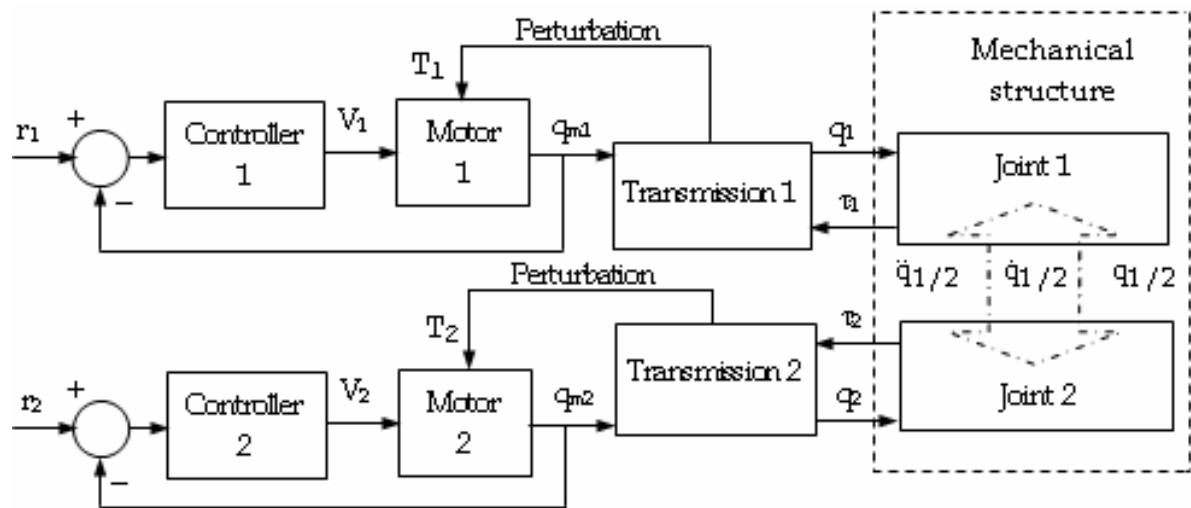


Fig. 10. The structural block scheme of the tracking system

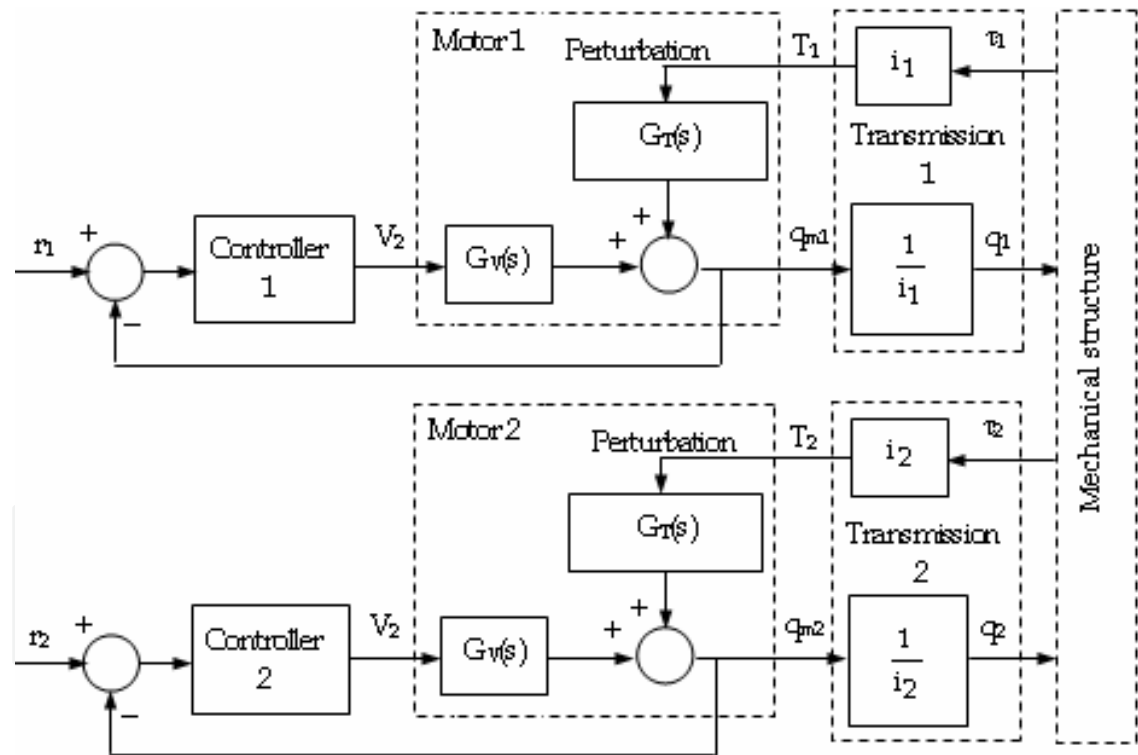


Fig. 11. The detailed control scheme

These relations lead to the detailed model shown in figure 11. Considering the numeric values from table 1, we obtained the following results for the transfer functions (G_V , and G_T respectively):

$$G_V(s)=\frac{1511}{s^3+430.8s^2+845.3s},\;G_T(s)=\frac{4291.84s+6866.95}{s^3+430.8s^2+845.3s}\tag{6}$$

Using the mentioned control strategy (see figure 11) the plant transfer function is $G_V(s)$. From (6) we can extract the following observations: in order to obtain a zero error for the unperturbed control loop, because of the zero-pole, it is appropriate to use a proportional controller; in order to reject a constant perturbation we will use the diagram transformations presented in figure 12 and the final value theorem (7):

$$q_m(\infty) = \lim_{s \rightarrow 0} s \cdot \frac{1}{s} \cdot \frac{G_T}{1 + G_V G_C} \quad (7)$$

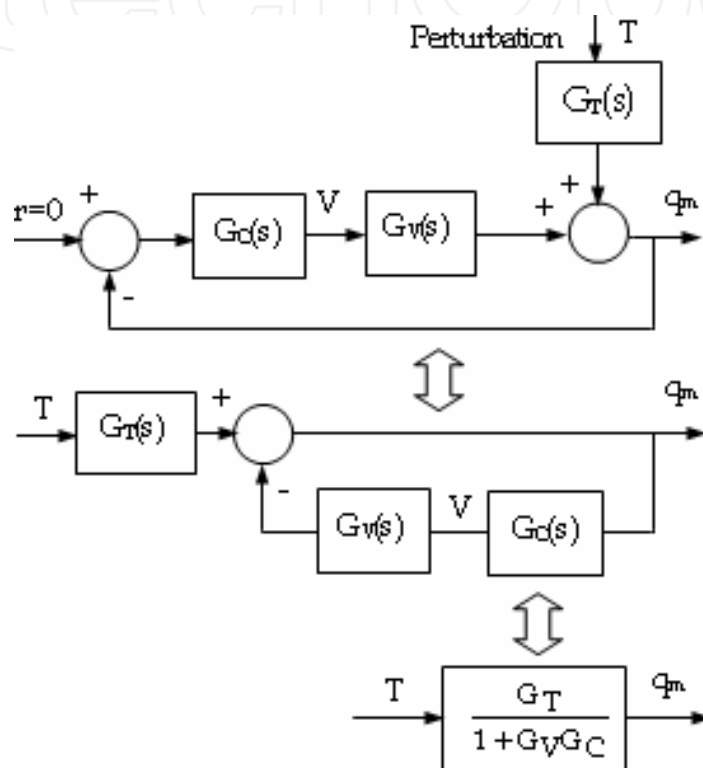


Fig. 12. The equivalent diagram

This result underlines that:

- using a proportional controller we can not reject the error caused by a constant perturbation:

$$q_m(\infty) = \frac{4.54}{K} \quad (8)$$

- for rejecting the perturbation effect ($q_m(\infty)=0$) we must use a controller which has a zero pole;
- the plant poles are:

$$\begin{cases} p_1 = 0 \\ p_2 = -1.9712 \\ p_3 = -428.8288 \end{cases} \quad (9)$$

- the step response of the control system is presented in figure 13.

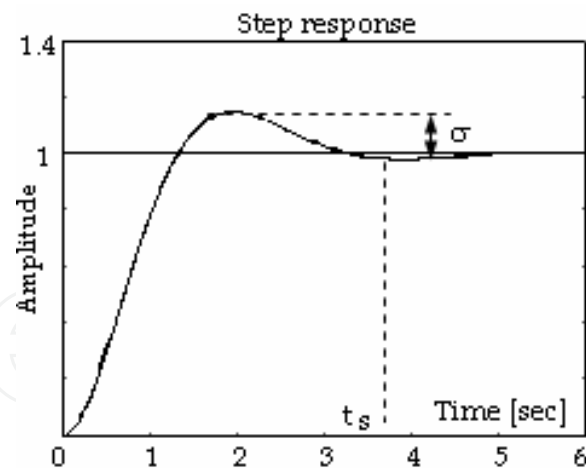


Fig. 13. The indicial response of the motor

Analyzing this result we obtain that the overshooting is $\sigma \cong 20\%$ and the transient regime duration is $t_s \cong 4s$. For the tracker control the recommended values are $\sigma < 5\%$, $t_s < 1s$. Meanwhile we will model the perturbations $T_{1/2}$ caused by the resistant torques in joints ($\tau_{1/2}$) with a step signal because these are bounded.

In conclusion:

- the tracking system is a complex system composed from three parts: the actuator, the gear transmission, and the mechanical structure of the tracker;
- the control strategy replace the use the actuator as the plant and consider the other mentioned subsystems perturbations source;
- the perturbations are bounded;
- for errors rejecting we will need a controller with a pole in origin;
- using the step response of the plant we have established the new transient response parameters.

For the controller synthesis in the state space we will adopt the following state vector:

$$x = [q \quad \dot{q} \quad i] \quad (10)$$

where q is the angular position, \dot{q} - is the angular velocity, i - the current intensity.

Using the mentioned state vector, the DC motor dynamic model is:

$$\dot{x} = \begin{bmatrix} 0 & 1 & 0 \\ 0 & -\frac{b}{J} & \frac{K_M}{J} \\ 0 & -\frac{K_b}{L} & -\frac{R_a}{L} \end{bmatrix} \cdot x + \begin{bmatrix} 0 \\ 0 \\ \frac{1}{L} \end{bmatrix} \cdot u + \begin{bmatrix} 0 \\ -\frac{1}{J} \\ 0 \end{bmatrix} \cdot T \quad (11)$$

$$y = [1 \quad 0 \quad 0] \cdot x$$

and by replacing the numerical values for the parameters (see table 1) we obtain:

$$\dot{x} = \begin{bmatrix} 0 & 1 & 0 \\ 0 & -429.1845 & 755.3648 \\ 0 & -0.21 & -1.6 \end{bmatrix} \cdot x + \begin{bmatrix} 0 \\ 0 \\ 2 \end{bmatrix} \cdot u + \begin{bmatrix} 0 \\ -4291.8 \\ 0 \end{bmatrix} \cdot T \quad (12)$$

$$y = [1 \quad 0 \quad 0] \cdot x$$

We can split this model in two parts:

- the unperturbed part:

$$\begin{aligned}\dot{x} &= \begin{bmatrix} 0 & 1 & 0 \\ 0 & -429.1845 & 755.3648 \\ 0 & -0.21 & -1.6 \end{bmatrix} \cdot x + \begin{bmatrix} 0 \\ 0 \\ 2 \end{bmatrix} \cdot u \\ y &= \begin{bmatrix} 1 & 0 & 0 \end{bmatrix} \cdot x\end{aligned}\tag{13}$$

- the perturbation effect:

$$\begin{aligned}\dot{x} &= \begin{bmatrix} 0 & 1 & 0 \\ 0 & -429.1845 & 755.3648 \\ 0 & -0.21 & -1.6 \end{bmatrix} \cdot x + \begin{bmatrix} 0 \\ -4291.8 \\ 0 \end{bmatrix} \cdot T \\ y &= \begin{bmatrix} 1 & 0 & 0 \end{bmatrix} \cdot x\end{aligned}\tag{14}$$

The simulation of the result is realized using the scheme shown in figure 14. In the controller synthesis we have used the Ackerman algorithm. For the imposed transient response parameters we have obtained the following control gains: $K=[5.9309 \quad 106.6441 \quad -187.3923]$; $k_i = 16.94$; the simulation of this result is shown in table 2.

Using this result, we can simulate the behaviour of the tracking system. In order to do this we must construct a block diagram (fig. 15) composed by the control loop and also by the perturbation source (the gear transmission and the tracker structure). In figure 15 we have used the following blocks: qd1/2 - the desired angular position of the tracker; motor 1/2 - the DC motors models; perturbation 1/2 - the perturbations models; mechanical device - the block that contain the mechanical structure of the tracking mechanism - see figure 8 (this block is used for determining the motor torques, and it works in inverse dynamics regime); ddq1/2 - the accelerations computation blocks. Using this simulation diagram we have obtained the results presented in table 3.

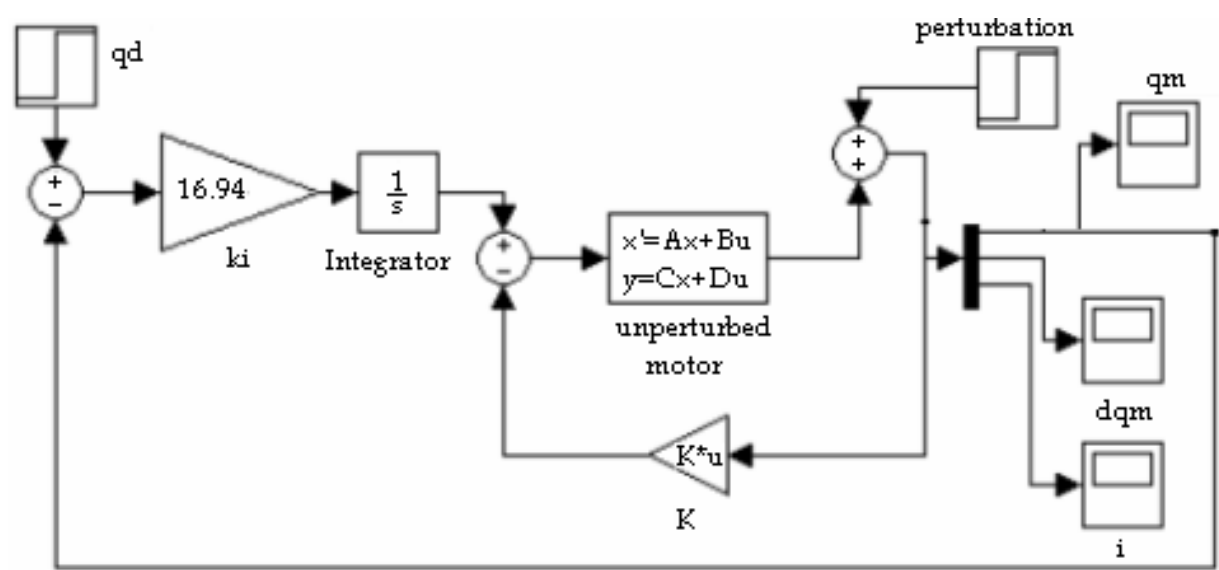


Fig. 14. The control scheme of the DC motor

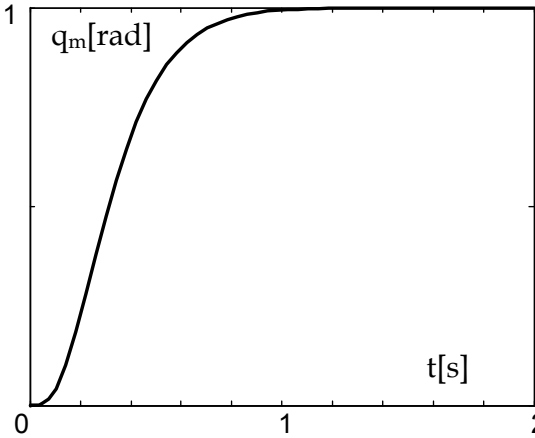
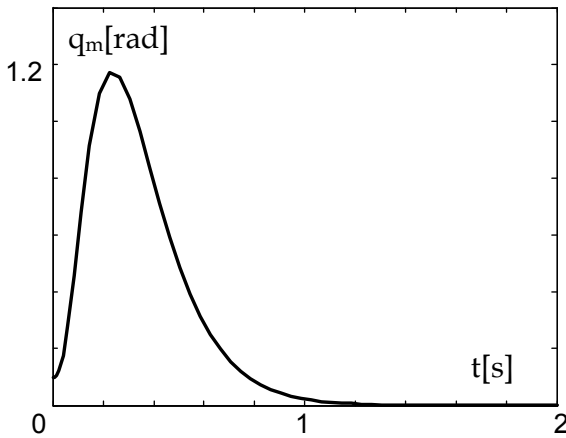
Indicial response	Eliminating the perturbation
	
qd is a step signal and the perturbation is zero; the system react critical damped; the settling time is 1 sec	qd is zero; the perturbation is a step signal

Table 2. The simulation of the result for the DC motor

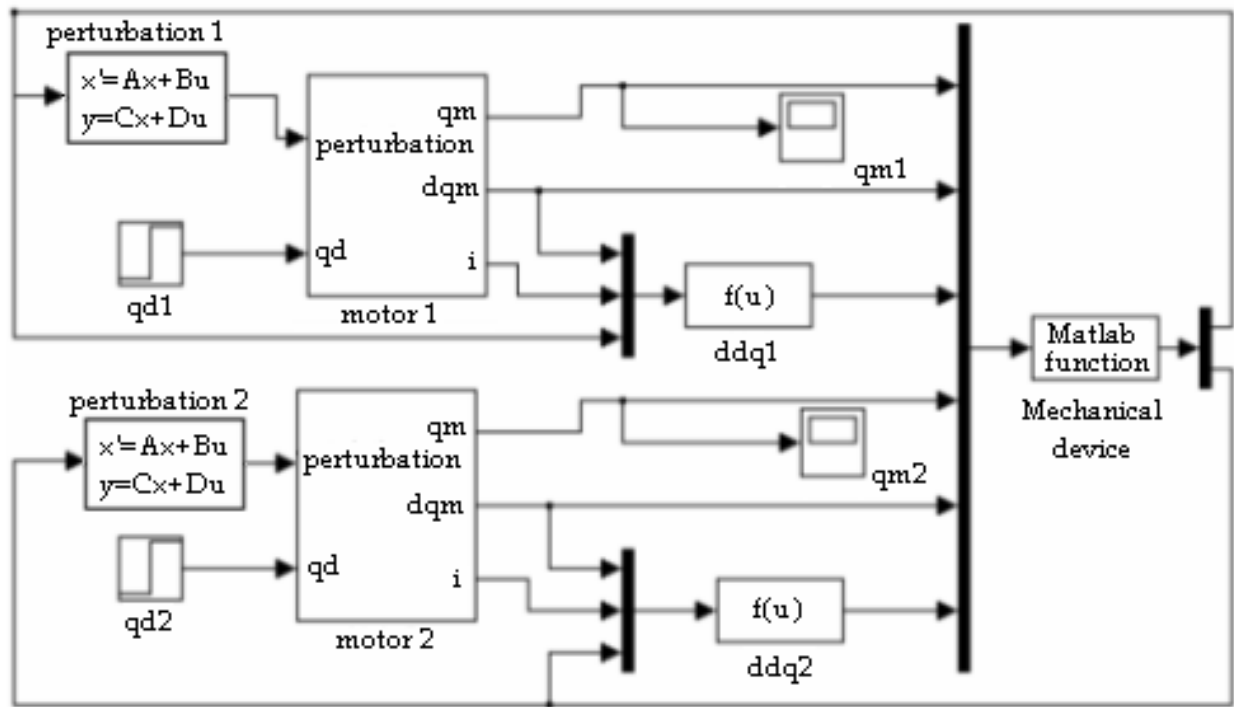


Fig. 15. The control diagram of the tracking mechanism (MATLAB)

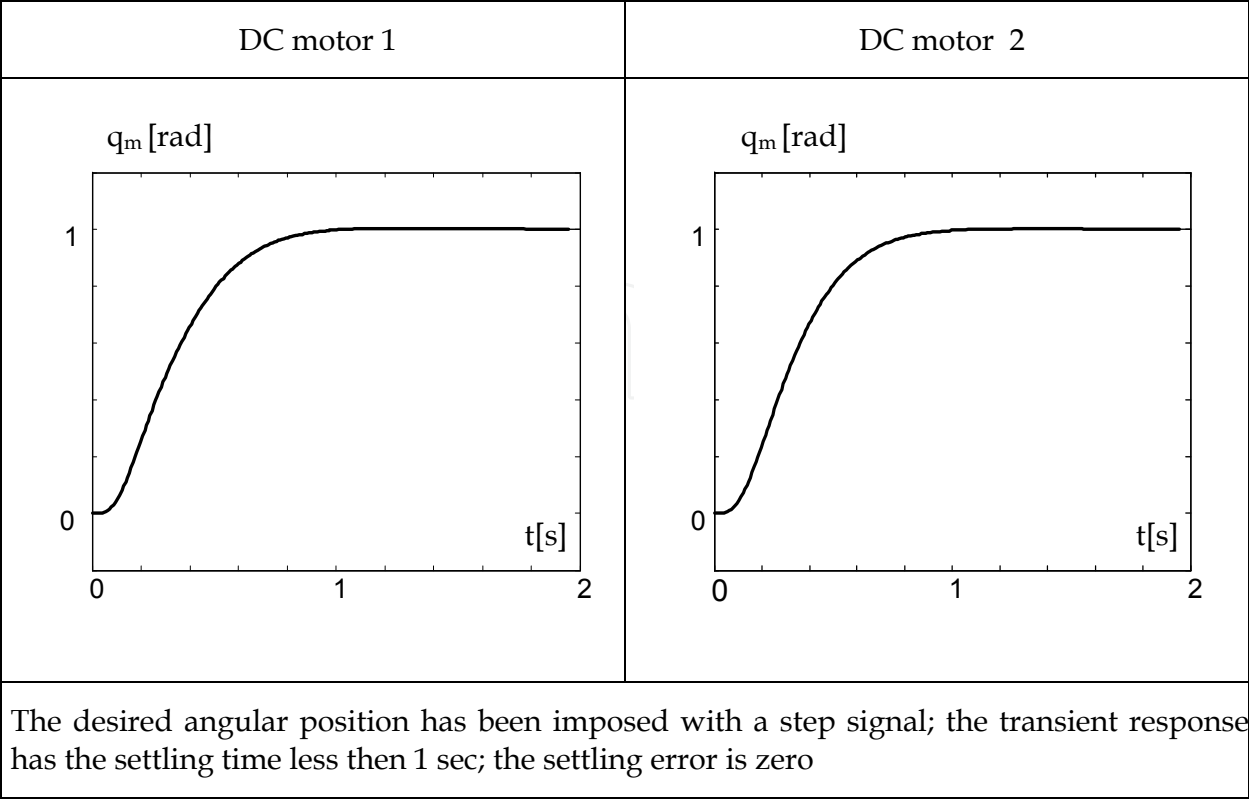


Table 3. The angular positions of the DC motors

In the next step, for finishing the simulation diagram of the mechatronic tracking system in the concurrent engineering concept, in the control diagram there will be integrated the MBS model of the mechanical system, which it was developed in ADAMS/View (see fig. 5); this model replaces the MATLAB function (i.e. the mechanical device from figure 15). The objective is to control the angular positions (for the DC motors which drive the daily and seasonal motions), which are perturbed with the motor torques. For connecting the mechanical model (ADAMS) with the electronic control system (MATLAB), the input & output parameters have been defined. The daily & seasonal angles of the PV panel (i.e. the angular positions) represent the input parameters in the MBS mechanical model. The outputs transmitted to the controller are the motor torques generated by the DC motors. For the input state variables, the run-time functions are 0.0 during each step of the simulation, because the variables will get their values from the control application. The run-time functions for these variables are VARVAL(daily_angle), and VARVAL(seasonal_angle), where VARVAL is a specific function that returns the value of the given variable. In other words, the input daily & seasonal angles get the values from the input variables. For the output state variables, the run-time functions return the sum of torques at locations. The next step is for exporting the ADAMS plant files for the control application. The Plant Inputs refer the input state variables (daily & seasonal angles), and the Plant Outputs refer the output state variables (daily & seasonal motor torques). ADAMS/Controls save the input and output information in a specific file for MATLAB (*.m); it also generates a command file (*.cmd) and a dataset file (*.adm), which will be used during the simulation. With these files, the control diagram can be developed, in order to complete the link between the mechanical and actuating - control systems. For beginning, the .m file is loaded in the MATLAB command line, and then, for creating the MSC ADAMS block diagram,

there is a special command, namely *adams_sys*. This builds a new model in Simulink (*adams_sys.mdl*), which contains the MSC.Software S-Function block representing the non-linear MSC.ADAMS model (i.e. the mechanical system). The *ADAMS_sub* block is created based on the information from the *.m* file (Alexandru, 2008).

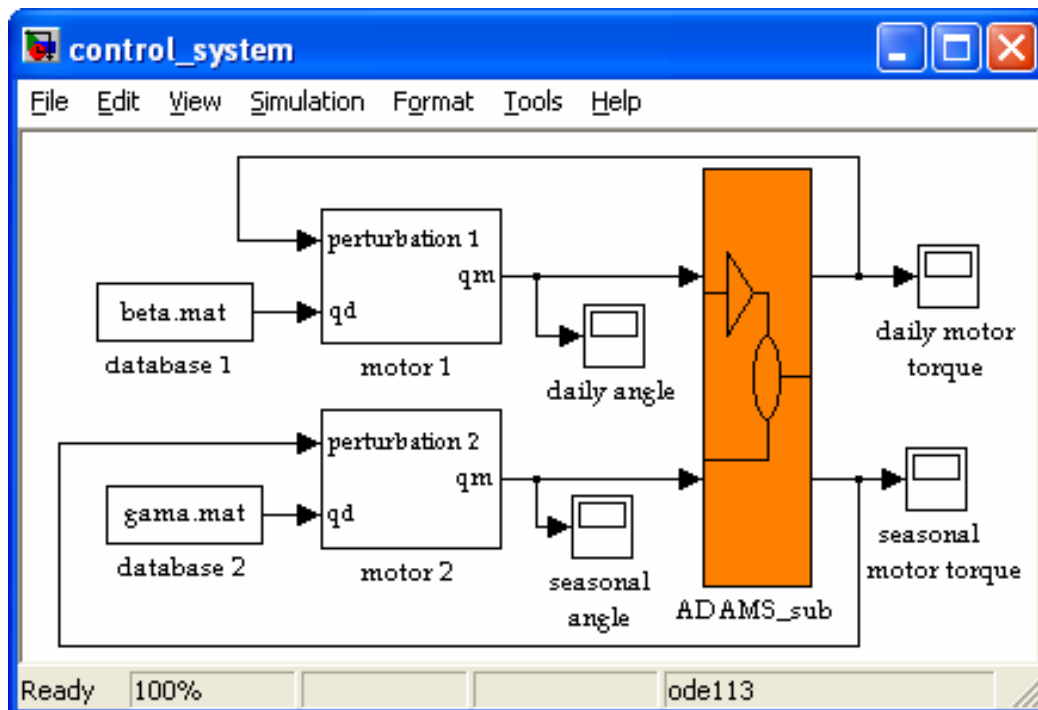


Fig. 16. The control system in the concurrent engineering concept (MATLAB + ADAMS)

Finally, the construction of the controls system block diagram (fig. 16) is made by integrating the *ADAMS_sub* block, the DC motors blocks, and the databases blocks containing the desired trajectory of the panel (for the daily & seasonal angles). To set the simulation parameters (e.g. the solver type, the communication interval, the number of communications per output step, the simulation & animation model), the MSC.ADAMS Plant Mask is used. In this way, ADAMS accepts the control inputs from MATLAB and integrates the mechanical model in response to them. At the same time, ADAMS provides the motor torques for MATLAB to integrate the control model.

5. Analyzing & optimizing the virtual prototype

The photovoltaic panel can be rotated without brakes during the day-light, or can be discontinuously driven (step-by-step motion), usually by rotating the panel with equal steps at every hour. Obviously, the maximum incident solar radiation is obtained for the continuous motion in the entire angular field (from -90° at sunrise, to $+90^\circ$ at sunset), but in this case the operating time of the system/motor is high. In our vision, the strategy for optimizing the motion law of the tracking system aims to reduce the angular field of the daily motion and the number of actuating operations, without significantly affecting the incoming solar energy, and to minimize the energy consumption for realizing the tracking. The energy produced by the PV panel depends on the quantity of incident solar radiation, the active surface of the panel, as well as the panel's efficiency. The incident radiation, which is normal to the active surface, is given by the relation:

$$G_I = G_D \cdot \cos i \quad (15)$$

where G_D is the direct terrestrial radiation, and i - the angle of incidence. The direct radiation is established using the next equation (Meliß, 1997):

$$G_D = G_0 \exp \left(- \frac{T_R}{0.9 + 9.4 \cdot \sin \alpha} \right) \quad (16)$$

with the following components:

$$G_0 = \overline{G}_0 \cdot (1 + 0.0334 \cdot \cos x) \quad (17)$$

$$x = 0.9856^\circ \cdot n - 2.72^\circ \quad (18)$$

$$\alpha = \sin^{-1} (\sin \delta \cdot \sin \varphi + \cos \delta \cdot \cos \varphi \cdot \cos \omega) \quad (19)$$

$$\omega = 15^\circ \cdot (12 - T) \quad (20)$$

where G_0 is the extraterrestrial radiation, \overline{G}_0 - the solar constant (1367 W/m^2), n - the day number during a year, T_R - the distortion factor, which depends on the month and the geographic region, α - the solar altitude angle, δ - the solar declination, φ - the location latitude, ω - the solar hour angle, and T - the local time.

The angle of incidence is determined from the scalar product of the sunray vector and the normal vector on panel,

$$i = \cos^{-1} (\cos \beta \cos \beta^* \cos (\gamma - \gamma^*) + \sin \beta \sin \beta^*) \quad (21)$$

$$\beta = \sin^{-1} (\cos \delta \cdot \sin \omega) \quad (22)$$

$$\gamma = \sin^{-1} \left(\frac{\cos \alpha \cdot \cos \psi}{\cos \beta} \right) \quad (23)$$

$$\psi = (\sin \omega) \cos^{-1} \left(\frac{\sin \alpha \cdot \sin \varphi - \sin \delta}{\cos \alpha \cdot \cos \varphi} \right) \quad (24)$$

in which β and γ are the diurnal & seasonal angles of the sunray, β^* and γ^* - the daily & elevation angles of the panel, and the ψ - the azimuth angle.

It has been demonstrated that for every month there is one day whose irradiation is equal to the monthly average: it is the day in which the declination equals the mean declination of the month (Sorichetti & Perpinan, 2007). Due to this consideration, a noticeable facilitation is introduced in the computing calculation, considering just the mean days of each month instead of the 365 days of the year.

This work presents the exemplification for the summer solstice path of the Sun. The situation is similar for any period of the year: the energy gain is not affected by the variation of the radiation intensity because the gain is obtained from the difference between a tracked panel energy output and a non-tracked panel energy output. In these conditions, the numeric simulations were performed considering the Braşov geographic area, with the following specific input data: $\varphi=45.5^\circ$, $\delta=23.45^\circ$, $n=172$, $T \in [5.579, 21.059]$, $T_R=4.2$, $\gamma^*=22.05^\circ$.

For identifying the optimum angular field of the daily motion, we have considered the correlation between the motion amplitude and the local solar time, for obtaining symmetric revolutive motions relative to the solar noon position ($\beta^*=0$). The analysis has been performed for the following tracking cases: (a) $\beta^*\in[-90^\circ, +90^\circ]$, $T\in[5.579, 21.059]$ - the maximum motion interval; (b) $\beta^*\in[-75^\circ, +75^\circ]$, $T\in[6.869, 19.769]$; (c) $\beta^*\in[-60^\circ, +60^\circ]$, $T\in[8.159, 18.479]$; (d) $\beta^*\in[-45^\circ, +45^\circ]$, $T\in[9.449, 17.189]$; (e) $\beta^*\in[-30^\circ, +30^\circ]$, $T\in[10.739, 15.899]$; (f) $\beta^*\in[-15^\circ, +15^\circ]$, $T\in[12.029, 14.609]$; (g) $\beta^*=0$, $T\in[5.579, 21.059]$ - the fixed (non-tracked) system. In this study, we considered that the PV panel is rotated without brakes (continuous motion). The computations have been made using the above-presented mathematic model, obtaining in this way the incident radiation for the considered cases. Integrating the incident radiation curves (shown in figure 17), and taking into account the active surface (1.26 m²) and the conversion efficiency of the panel (15%), we have obtained the quantity of electric energy produced by the PV system. Afterwards, the energy consumption for realizing the motion laws was determined by using the virtual prototype of the tracking system (see section 4).

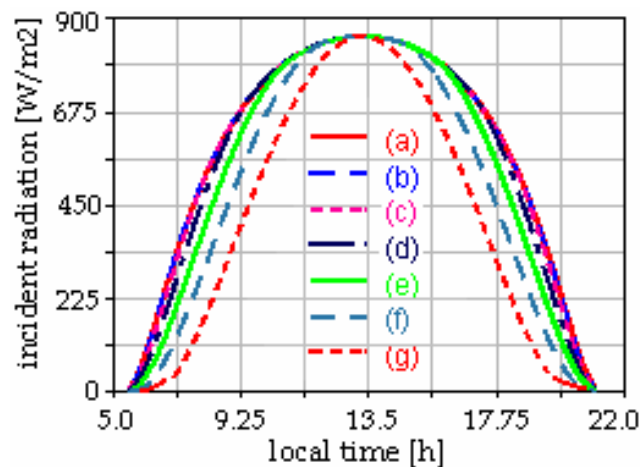


Fig. 17. The incident radiation curves

For the energy consumption, there is also considered the return of the tracking mechanism in the initial position (east/sunshine) after the sunset, which is performed with 10 degrees per minute (0.016667 hours). In this way, the energy balance was performed, the results being systematized in the table 4 (the energy gain is computed relative to the fixed panel case). Analyzing these results, we consider that the optimal angular field for the daily motion of the panel, in the summer solstice day, is $\beta^*\in[-60^\circ, +60^\circ]$, in which there is the maximum energy gain.

β^*	E_T [Wh/day]	E_C [Wh/day]	Gain [%]
$[-90^\circ, +90^\circ]$	1740.88	44.09	37.87
$[-75^\circ, +75^\circ]$	1739.40	37.01	38.32
$[-60^\circ, +60^\circ]$	1726.44	17.64	38.84
$[-45^\circ, +45^\circ]$	1685.62	12.77	35.92
$[-30^\circ, +30^\circ]$	1598.91	5.84	29.44
$[-15^\circ, +15^\circ]$	1449.61	1.49	17.66
0°	1230.73	-	-

Table 4. The energy balance for different angular fields of the daily motion

Afterwards, in the optimal angular field, we have evaluated different step-by-step tracking strategies. The objective is to minimize the operating time, which is important for the durability & reliability of the tracking system. In these terms, we have developed - analyzed six tracking cases, depending on the number of steps (in consequence, the step dimension - $\Delta\beta^*$) for realizing the optimum angular field: 12 steps ($\Delta\beta^*=10^\circ$), 10 steps ($\Delta\beta^*=12^\circ$), 8 steps ($\Delta\beta^*=15^\circ$), 6 steps ($\Delta\beta^*=20^\circ$), 4 steps ($\Delta\beta^*=30^\circ$), 2 steps ($\Delta\beta^*=60^\circ$); in each case, the angular velocity for the motion steps is 10 degrees per minute.

One of the most important problems in the step-by-step tracking is to identify the optimum actuating time, in which the motion step has to be performed. In paper, the solution to this problem is obtained by developing an algorithm based on the following phases: the optimal angular field was segmented into the intermediary positions, depending on the step dimension for each case (e.g. for 4 steps there are the following positions: $\beta^* = \{\pm 60^\circ, \pm 30^\circ, 0^\circ\}$), and the incident radiation curves have been consecutively obtained considering the panel fixed in these positions during the day-light; analyzing these curves, we have identified the moment in which the value of the incident radiation for a certain position k become smaller than the value in the next position $k+1$; in this moment, the motion step is performed; the analysis continues with the next pair of positions $k+1$ and $k+2$, and so on. For example, in the figure 18 there are presented the diagrams for the 4-steps tracking case. Because there is a symmetrical motion relative to the noon position ($T=13.319$ - local time), the actuating moments are also symmetrically disposed (I-IV, II-III).

For the considered step-by-step tracking cases, the results of the energy balance are systematized in the table 5. According with these results, by using the above-presented algorithm for configuring the step-by-step orientation, we obtained values closed-by the

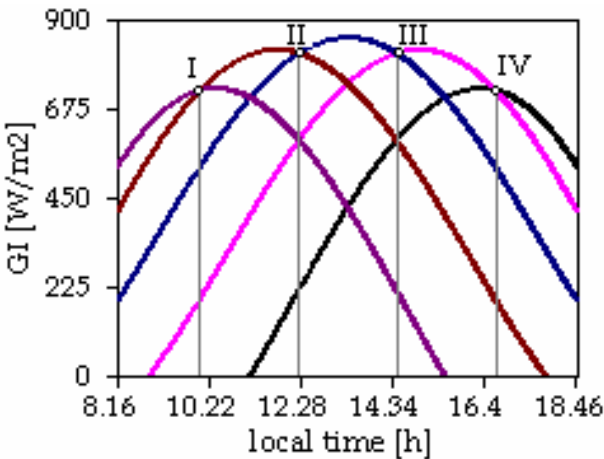


Fig. 18. The optimum actuating time

No. of steps	E_T [Wh/day]	E_C [Wh/day]	Gain [%]
12	1722.19	20.78	38.24
10	1719.72	19.99	38.11
8	1718.35	19.47	38.04
6	1715.39	19.00	37.84
4	1706.92	18.23	37.21
2	1670.97	17.65	34.34

Table 5. The energy balance for the step-by-step tracking cases

continuous motion case, and this demonstrates the viability of the adopted optimization strategy. As we can see, the energy consumptions for realizing the step-by-step motion laws are greater than the energy consumption for the continuous motion, and this because of the over-shootings that appear when the motor is turned-on/off.

Similar studies have been performed for different periods/days, obtaining in this way the optimum motion laws during the year.

The final aspect for this study is to refine the tracking system by adding flexible bodies. The modelling of the mechanical structure of the tracking system with finite elements has two main objectives: identifying the eigenshapes and eigenfrequencies of the system, which are useful to avoid the resonance phenomenon due to the action of the external dynamic loads (as wind or earthquake); identifying the maximum deformabilities and the equivalent stresses, depending on the action of the external factors and on the position of the structure. In paper, the analysis of the structure is made for different values of the daily position of the panel, in the above-obtained optimum field, $\beta \in [-60^\circ, +60^\circ]$, the elevation being fixed at 22.05° (for the summer solstice day, in Braşov geographic area). The external load is materialized by forces and pressures which are produced by a 90 km/h wind speed which is acting on the structure; this speed generates a pressure of 1200 MPa on the panel's surface.

For creating the finite element model of the tracking system, we used the specific ADAMS/AutoFlex module, which automatically mesh the geometries imported from CAD system. In these terms, analyzing the refined virtual prototype of the tracking system, we obtained the following results: the variation of the eigenfrequencies with the daily position angle is insignificant from quantitative point of view; the maximum values of the equivalent stresses (von Misses), which appear in the rotational joints of the structure, are less than the admissible resistance values (90...120 MPa), and this assures the mechanical resistance condition (the maximum value is 71 MPa); the maximum value of the deformability is small ($< 0.08\text{mm}$), and this ensures proper functioning of the system. Among the specific results, in figure 19 there are shown the variations of the von Misses equivalent stresses (a) and deformations (b) fields, as well as the eigenfrequencies (c), for the daily angle $\beta^* = -60^\circ$.

6. Conclusions

The application is a relevant example regarding the implementation of the virtual prototyping tools in the design process of the photovoltaic tracking systems. One of the most important advantages of this kind of simulation is the possibility to perform virtual measurements in any point or area of the tracking system, and for any parameter (for example motion, force, and/or energy). Using the virtual prototyping platform, we are able to optimize the mechanical structure of the tracking mechanism, choose the appropriate actuators, design the optimal controller, optimize the motion law, and perform the energy balance of the photovoltaic system. In this way, we are much better equipped to manage the risks inherent in the product development cycle.

Connecting the electronic control system and the mechanical device at the virtual prototype level (i.e. the concurrent engineering concept), the physical testing process is greatly simplified, and the risk of the control law being poorly matched to the real tracking system is eliminated. At the same time, integrating the finite element model in the multibody system analysis, we can quickly build a parametric flexible body representation of a component, analyze the system, make changes to the flexible body and evaluate the effect of the changes, all within the MBS environment.

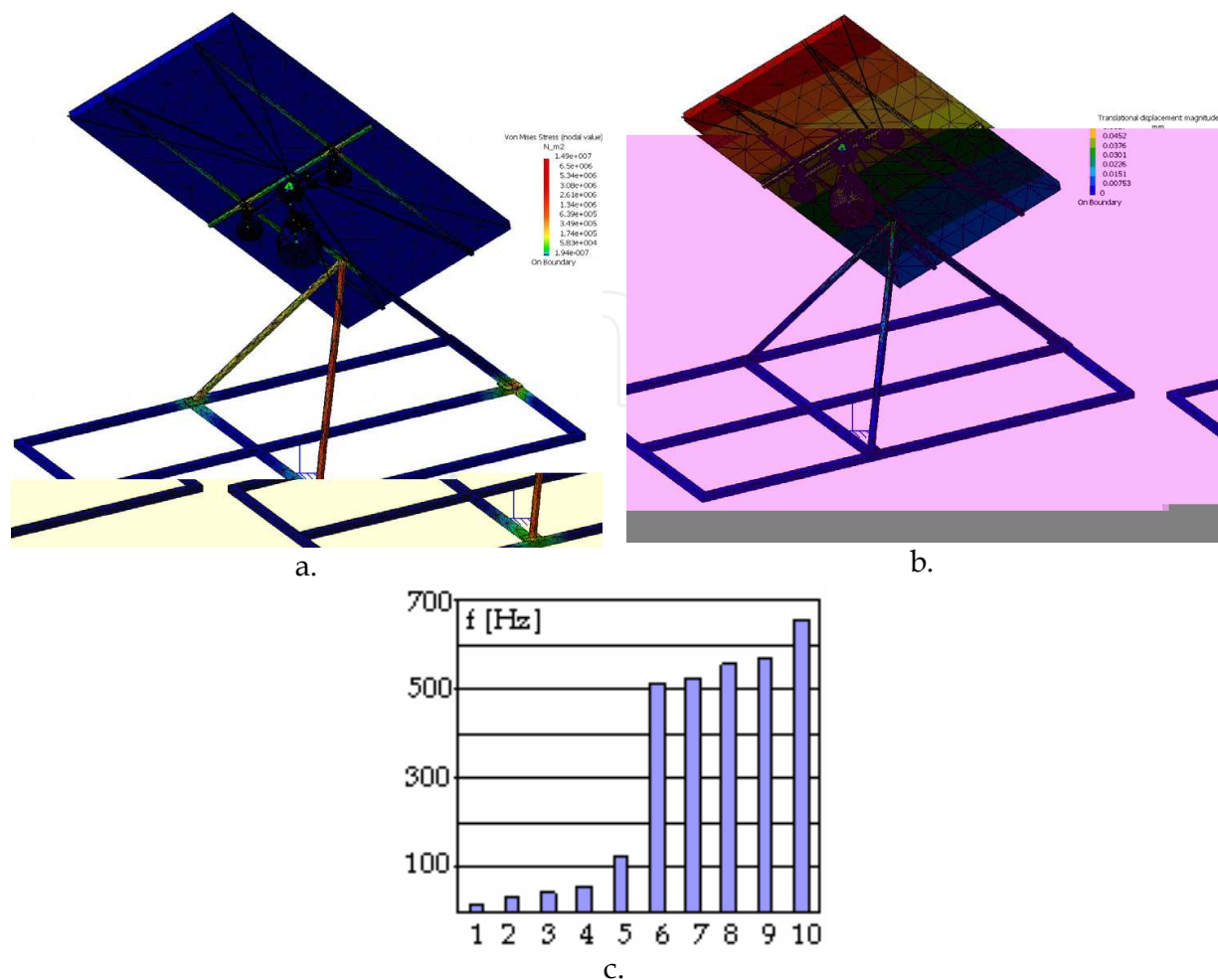


Fig. 19. Specific results of the finite element analysis (flexible multibody system)

The optimization strategy of the motion law, which is based-on the minimization of the angular field for the daily motion and the minimization of the number of actuating operations, leads to an efficient PV system, without developing expensive hardware prototypes. Thus, the behavioural performance predictions are obtained much earlier in the design cycle of the tracking systems, thereby allowing more effective and cost efficient design changes and reducing overall risk substantially.



Fig. 20. The physical prototype of the polar tracking system

The tracking system has been manufactured (fig. 20) and it will be tested in the Centre Product Design for Sustainable Development from Transilvania University of Braşov, creating a real perspective for the research in the field. This will allow a relevant comparison between the virtual prototype analysis and the data achieved by measurements; the results of the comparative analysis will be presented in a future paper.

7. References

- Abdallah, S. & Nijmeh, S. (2004). Two-axes sun tracking with PLC control. *Energy Conversion and Management*, Vol. 45, No. 11-12, 1931-1939, ISSN 0196-8904
- Alata, M.; Al-Nimr, M.A. & Qaroush, Y. (2005). Developing a multipurpose sun tracking system using fuzzy control. *Energy Conversion and Management*, Vol. 46, No. 7-8, 1229-1245, ISSN 0196-8904
- Alexandru, C. (2008). The mechatronic model of a photovoltaic tracking system. *International Review on Modelling and Simulations - IREMOS*, Vol. 0, No. 0, 64-74, ISSN 1974-9821
- Alexandru, C. & Comsit, M. (2008). The energy balance of the photovoltaic tracking systems using virtual prototyping platform, *Proceedings of the 5th International Conference on the European Electricity Market - EEM*, pp. 1-6, ISBN 978-1-4244-1743-8, Lisbon, May 2008, IEEE/PES
- Alexandru, C. & Pozna, C. (2007). Different tracking strategies for optimizing the energetic efficiency of a photovoltaic system, *Proceedings of the 16-th IEEE International Conference on Automation, Quality and Testing, Robotics - AQTR/THETA*, Vol. 3, pp. 434-439, ISBN 978-1-4244-2576-1, Cluj-Napoca, May 2008, IEEE/TTTC
- Baltas, P.; Tortoreli, M. & Russel, P. (1986). Evaluation of power output for fixed and step tracking photovoltaics. *Solar Energy*, Vol. 37, No. 2, 147-163, ISSN 0038-092X
- Canova, A.; Giaccone, L. & Spertino, F. (2007). Sun tracking for capture improvement, *Proceedings of the 22nd European Photovoltaic Solar Energy Conference - EUPVSEC*, pp. 3053-3058, ISBN 3-936338-22-1, Milan, September 2007, WIP-Renewable Energies
- Chojnacki, J.A. (2005). Application of fuzzy logic neural network controllers in PV systems, *Proceedings of the 20th European Photovoltaic Solar Energy Conference - EUPVSEC*, pp. 2269-2272, ISBN 3-936338-19-1, Barcelona, June 2005, WIP-Renewable Energies
- Clifford, M.J. & Eastwood, D. (2004). Design of a novel passive tracker. *Solar Energy*, Vol. 77, No. 3, 269-280, ISSN 0038-092X
- Comsit, M. & Visa, I. (2007). Design of the linkages-type tracking mechanisms by using MBS method, *Proceedings of the 12th IFToMM World Congress*, pp. 582-587, ISBN 7-89492-107-6, Besancon, June 2007, IFToMM
- Dobon, F.; Lugo, A. & Monedero, J. (2003). First results of the tetra-track system and control electronics, *Proceedings of the 3rd World Conference on Photovoltaic Energy Conversion - WCPEC*, pp. 2050 - 2053, ISBN 4-9901816-0-3, Osaka, May 2003, IEEE
- Garcia de Jalón, J. & Bayo, E. (1994). *Kinematic and Dynamic Simulation of Multibody Systems*, Springer-Verlag, ISBN 0-387-94096-0, New-York

- Goswami, Y.; Kreith, F. & Kreider, J. (2000). *Principles of Solar Engineering*, Taylor & Francis, ISBN 1-56032-714-6, Philadelphia
- Haug, E.; Choi, K.; Kuhl, J. & Vargo, J. (1995). Virtual prototyping for design of mechanical systems. *Journal of Mechanical Design*, Vo. 117, No. 63, 63-70, ISSN 1050-0472
- Hoffmann, A.; Frindt, H.; Spinnler, M.; Wolf, J.; Sattelmayer, T. & Hartkopf, T. (2008). A systematic study on potentials of PV tracking modes, *Proceedings of the 23rd European Photovoltaic Solar Energy Conference - EUPVSEC*, pp. 3378-3383, ISBN 3-936338-24-8, Valencia, September 2008, WIP-Renewable Energies
- Karimov, K.; Saqib, M. & Akhter, P. (2005). A simple photovoltaic tracking system. *Solar Energy*, Vol. 87, No. 1-4, 49-59, ISSN 0038-092X
- Koay, C.W. & Bari, S. (1999). Intermittent tracking of flat plate collectors, *Proceedings of the World Renewable Energy Congress - WREC*, pp. 79-82, ISBN 9-8399-9481-6, Kuala Lumpur, June 1999, World Renewable Energy Network
- Meliß, M. (1997). *Regenerative Energiequellen*, Springer-Verlag, ISBN 3-540-63218-2, Berlin
- Narvarte, L. & Lorenzo, E. (2007). Tracking gains and ground cover ratio, *Proceedings of the 22nd European Photovoltaic Solar Energy Conference - EUPVSEC*, pp. 3153-3156, ISBN 3-9363-3822-1, Milan, September 2007, WIP-Renewable Energies
- Pahl, G. & Beitz, W. (1996). *Engineering Design*, Springer-Verlag, ISBN 3-5401-9917-9, London
- Reda, I. & Andreas, A. (2004). Solar position algorithm for solar radiation applications. *Solar Energy*, Vol. 76, No. 5, 577-589, ISSN 0038-092X
- Roth, P.; Georgiev, A. & Boudinov, H. (2004). Design and construction of a system for sun-tracking. *Renewable Energy*, Vol. 29, No. 3, 393-402, ISSN 0960-1481
- Rubio, F.R. & Aracil, J. (1997). Design of a combined tracking control system. *Control Engineering Practice*, Vol. 5, No. 1, 23-31, ISSN 0967-0661
- Rubio, F.R.; Ortega, M. & Gordillo, F. (2007). New control strategy for sun tracking. *Energy Conversion and Management*, Vol. 48, No. 7, 2174-2184, ISSN 0196-8904
- Ryan, R. (2001). *Functional Virtual Prototyping*, Mechanical Dynamics Inc. Press, Michigan
- Sala, G.; Pachon, D. & Anton, I. (2002). *Test, Rating and Specification of PV Concentrator Components and Systems*, Instituto de Energia Solar, Madrid
- Salmi, M.; Chegaar, M. & Mialhe, P. (2007). Modèles d'estimation de l'irradiation solaire globale au sol. *Revue Internationale d'Heliotechnique Energie - Environment*, No. 35, 19-24, ISSN 0378-1305
- Scharmer, K. & Greif, J. (2000). *The European Solar Radiation Atlas*, Ecole des Mines, Paris
- Schiehlen, W.O. (1997). Multibody systems - roots and perspectives. *Multibody Systems Dynamics*, Vol. 1, No. 2, 149-188, ISSN 1384-5640
- Sorichetti, R. & Perpignan, O. (2007). PV solar tracking systems analysis, *Proceedings of the 22nd European Photovoltaic Solar Energy Conference - EUPVSEC*, pp. 246-252, ISBN 3-9363-3822-1, Milan, September 2007, WIP-Renewable Energies
- Tiwari, G.N. (2002). *Solar Energy: Fundamentals, Design, Modeling and Applications*, Alpha Science Int. Ltd., ISBN 0-8493-2409-2, Pangbourne

- Tymvios, F.S.; Jacovides, C.P. & Scouteli, C. (2005). Comparative study of Angstrom's and artificial neural networks methodologies in estimating global solar radiation. *Solar Energy*, Vol. 78, No. 6, 752-762, ISSN 0038-092X
- Yazidi, A.; Betin, F. & Notton, G. (2006). Low cost two-axis solar tracker with high precision positioning, *Proceedings of the 1st International Symposium on Environment Identities & Mediterrance Area*, pp. 211-216, ISBN 1-4244-0231-X, Corte-Ajaccio, July 2006, IEEE

IntechOpen

IntechOpen



Motion Control

Edited by Federico Casolo

ISBN 978-953-7619-55-8

Hard cover, 590 pages

Publisher InTech

Published online 01, January, 2010

Published in print edition January, 2010

The book reveals many different aspects of motion control and a wide multiplicity of approaches to the problem as well. Despite the number of examples, however, this volume is not meant to be exhaustive: it intends to offer some original insights for all researchers who will hopefully make their experience available for a forthcoming publication on the subject.

How to reference

In order to correctly reference this scholarly work, feel free to copy and paste the following:

Cătălin Alexandru and Claudiu Pozna (2010). The Analysis and Optimization in Virtual Environment of the Mechatronic Tracking Systems Used for Improving the Photovoltaic Conversion, Motion Control, Federico Casolo (Ed.), ISBN: 978-953-7619-55-8, InTech, Available from: <http://www.intechopen.com/books/motion-control/the-analysis-and-optimization-in-virtual-environment-of-the-mechatronic-tracking-systems-used-for-im>

INTECH
open science | open minds

InTech Europe

University Campus STeP Ri
Slavka Krautzeka 83/A
51000 Rijeka, Croatia
Phone: +385 (51) 770 447
Fax: +385 (51) 686 166
www.intechopen.com

InTech China

Unit 405, Office Block, Hotel Equatorial Shanghai
No.65, Yan An Road (West), Shanghai, 200040, China
中国上海市延安西路65号上海国际贵都大饭店办公楼405单元
Phone: +86-21-62489820
Fax: +86-21-62489821

© 2010 The Author(s). Licensee IntechOpen. This chapter is distributed under the terms of the [Creative Commons Attribution-NonCommercial-ShareAlike-3.0 License](https://creativecommons.org/licenses/by-nc-sa/3.0/), which permits use, distribution and reproduction for non-commercial purposes, provided the original is properly cited and derivative works building on this content are distributed under the same license.

IntechOpen

IntechOpen